Phys. Status Solidi A **208**, No. 4, 749–753 (2011) / **DOI** 10.1002/pssa.201084015

physica status solidi a
www.pss-a.com
applications and materials science

Application of the electron probe microanalysis in nitride-based heterostructures investigation

Yana Kuznetsova*[,1], Marina Baidakova[1], Ekaterina Flegontova[1], Anton Kuznetsov[2], Alla Sitnikova[1], and Maria Zamoryanskaya[1]

[1] Ioffe Physico-Technical Institute, Polytekhnicheskaya 26, 194021 St. Petersburg, Russia
[2] St. Petersburg Academic University – Nanotechnology Research and Education Centre RAS, Khlopina Street 8/3, 194021 St. Petersburg, Russia

Received 3 July 2010, revised 29 December 2010, accepted 6 January 2011
Published online 26 January 2011

Keywords electron probe microanalysis, Monte-Carlo simulation, nanoscale layers, nitrides

* Corresponding author: e-mail yana@mail.ioffe.ru, Phone: +7 812 292 7382, Fax: +7 812 297 1017

The aim of this work was development of electron probe microanalysis (EPMA) technique suitable for composition determination of nanoscale layers. Proposed technique allows to determine the content of thin layers lying beneath the surface including single quantum wells (SQWs). The method is based on Monte-Carlo numerical simulations. Application of this technique to the nitride heterostructures with SQWs and multiple quantum wells (MQWs) was demonstrated. Peculiarities of the method are discussed.

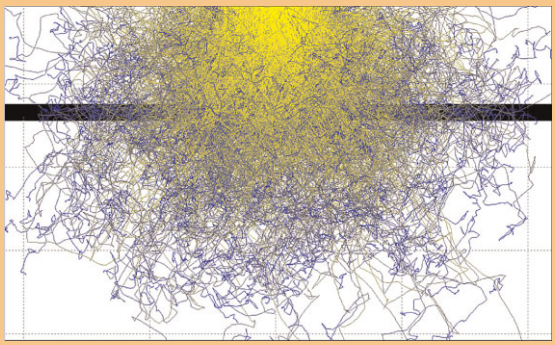

Electron trajectories in GaN sample with $In_{0.1}Ga_{0.9}N$ single quantum well. Simulation was made by Monte-Carlo method.

1 Introduction Despite the successfully application of GaN-based phosphorous-free light emitting devices problems of recombination mechanisms, phase separation, segregation and inhomogeneity in InGaN/GaN heterostructures are not fully understood. Further development of highly efficient devices demands investigation of obtained structures characteristics. Therefore, new methods and techniques are necessary for more detailed study.

One of popular techniques used in modern material science is electron probe microanalysis (EPMA) which is frequently used in scanning electron microscopes. However, this technique is overwhelmingly used for analysis of bulk samples or thick films (~500 nm) [1–3].

In our work, we revealed that such technique as EPMA can be a very useful tool for structures with single and multiple quantum wells (SQWs and MQWs) characterization. Since the depth of X-ray generation depends on the electron beam energy, it provides information on in-depth changes in the heterostructure composition in a range of 50 nm to 1 μm [4]. The method of electron beam energy variation applied for EPMA allows discovering of inhomogeneities in quantum well (QW) content distribution.

2 Experimental Two samples were investigated. The sample with SQW InGaN was grown by PAMBE [5], the sample with MQWs was grown by MOCVD. Both samples were grown on GaN buffer layer on c-Al_2O_3 substrate. Our measurements showed that because of the temperature gradient during growing process areas with different SQW content were formed in the first sample. Hereinafter, we compared parts of the SQW sample with highest (In-rich) and lowest (In-poor) indium content.

The samples were studied by electron microprobe analysis, local cathodoluminescence (CL), X-ray diffraction (XRD) and transmission electronic microscopy (TEM).

The composition of the SQW was determined by EPMA using electron microprobe analyzer 'Camebax' with wavelength spectrometers. The method of microanalysis matrix correction was used to calculate the composition. The characteristic line Lα for In (3.73 keV) was chosen for analysis. The intensity of In Lα characteristic X-ray emission from the InGaN nanoscale layer was measured with respect to the reference standard. Thick homogeneous epitaxial layer of InP with a known composition and thickness was used as a standard. The electron beam energy varied from 4 to 15 keV, the electron beam current was 50 nA. We increased counting time because of small layer thickness. The background was measured on GaN samples free of the analysed In element. Relative accuracy of measurements is up to the 10%.

The cathodoluminescent (CL) measurements were taken using original CL spectrometer installed into the optical microscope port of the Camebax electron microprobe [6]. The CL spectra were acquired at energy of electron beam 5 keV. All spectra were measured by the temperature of 77 and 300 K. The electron beam current was chosen in range of 0.1–100 nA.

TEM investigations were made at electron microscope EM-420 (energy of the electron beam 100 keV) and JEOL 2100 A (energy of electron beam 200 keV). Samples were prepared using standard ion beam thinning technique.

The XRD was studied using a D8 Discover X-ray diffractometer (Bruker AXS, Germany). A detailed analysis of the XRD patterns was performed by Leptos software package (Bruker).

3 Results and discussion

3.1 Monte-Carlo simulations for QW content determination In our measurements, we followed analogous method as for calculation of the barrier layer content in light emitting device structure [7]. However there were some differences. Briefly the procedure is following.

Differential electron flux density was calculated by Monte-Carlo simulation. Here, we applied the single scattering model. Physical models used in the Monte-Carlo calculation are described in detail in Ref. [7]. Differential electron flux density is related to the electron flux depth distribution. Knowing of the atomic shell ionization cross-section by electron excitation and X-ray linear absorption coefficient gives the possibility to evaluate the generation density of characteristic X-ray with regard to absorption of X-ray emission. If one integrates this expression by depth one receives the measured intensity of X-Ray by given probe energy E. Thus, at the energy E the intensity ratio of the analytical characteristic line in sample and standard (so-called K-ratio $K(E)$) is described by the equation:

$$K(E) = \frac{\int_0^\infty N(z)\varphi(z,E)\exp\left(-\int_0^z \mu(\tau)\mathrm{d}\tau \Big/ \cos\gamma\right)\mathrm{d}z}{\int_0^\infty N_{\mathrm{STAND}}\varphi_{\mathrm{STAND}}(z,E)\exp(-\mu_{\mathrm{STAND}}z/\cos\gamma)\mathrm{d}z}.$$

Here, the following notation was used: N is the concentration of atoms of the analysed element at depth z; φ the density of characteristic X-ray emission generation; μ the coefficient of linear absorption of the characteristic line and γ is the angle between the normal surface and the direction towards the X-ray detector.

In order to unambiguously reproduce the concentration profile it is necessary to assume the form of the function $N(z)$. In general if applying this technique for very thin nanoscale layers one can determine average indium atomic depth concentration in the layer only. In other words the product of absolute indium atomic concentration by thickness of the layer is measured by EPMA. So if a sample with MQWs is studied one has to know exact thickness of the QWs and barrier layers. If the layer is not continuous one should make some assumption concerning structure of the inhomogeneous layer.

3.2 EPMA measurements In Table 1 measured K-ratios of samples are shown. According to our results, three measurements of K-ratio by different energies are enough for correct calculation of QW content. It is better to choose such electron beam energies at which the maximum of X-ray generation is lying upper than QW, in the centre of the QW and lower than QW.

For the first time it was shown that the sensitivity of wavelength dispersive EPMA is enough for analysis of 5 nm thick single nanoscale layer. The content of SQW was calculated as $In_{0.08}Ga_{0.92}N$ in In-rich area and $In_{0.04}Ga_{0.96}N$ in In-poor area.

3.3 MQW structure For more precise determination of QW content additional precise information about the layer thickness was necessary.

We have obtained TEM image of MQW sample (Fig. 1). It is clearly seen that QWs have sharp interfaces. One can suppose that contribution of single large QWs in this structure is insignificant.

However, it was difficult to determine layer thicknesses according such TEM data precisely. Elastic strains contribute

Table 1 Measured K-ratios of the samples.

electron beam energy (keV)	K-ratio of In-rich SQW	K-ratio of In-poor SQW	K-ratio of MQW
4	0	0	–
5	0.0014	0.0005	–
6	0.0021	0.0009	0.034
7	0.0021	0.0011	0.028
8	0.0029	0.0012	0.026
9	0.0021	0.0011	–
10	0.0024	0.0014	0.016
11	0.0019	0.0013	–
12	0.0015	0.0008	0.013
13	0.0015	0.0008	–
14	0.0012	0.0008	–
15	0.0011	0.0004	–

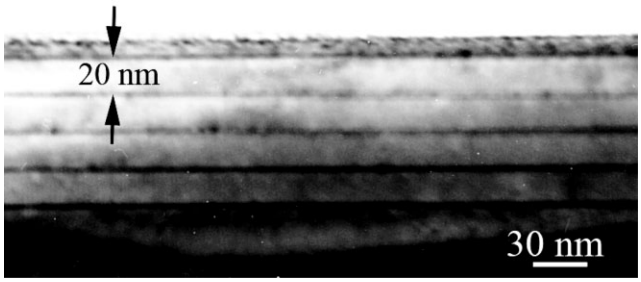

Figure 1 TEM image of the MQW structure.

to the microscope image that is particularly important factor in nitrides. Therefore, it is necessary to estimate error of TEM layer thickness determination, It was shown [8] that the relative accuracy of coherent QD radius determination can make up 15–20%. Moreover, TEM data characterize minor part of the sample rather then structure as a whole.

Therefore, we decided to use XRD data for layer thickness determination. Results of XRD curve fitting (Fig. 2) are shown in Table 2. One can see that exact compositions and thicknesses of each QW in MQW structure differ but the product of these parameters is constant.

We obtained XRD map to ensure that MQWs mainly consist of continuous QW layers (Fig. 3). In general, there is no possibility to obtain diffraction from disordered quantum dots (QDs) layer by common technique because of small relative QDs scattering volume [9]. However, if QDs stack in growing direction (*e.g.* in the multiple well structure) one can see additional diffusion scattering near superstructure reflections and additional peaks appearance [10]. Our results showed that there is no reflex widening in q_x direction or additional reflex ordering connected with QDs formation. Certainly we can not eliminate entirely QDs existence. However, QDs amount is less than experimental accuracy and QDs are not ordered. According to the XRD modelling results relative accuracy in QW thickness determination is up to 5%.

So, as it is showed in Table 2 EPMA results are in good agreement with XRD results.

CL spectra of the MQW structure are shown at Fig. 4. We have calculated the energy band structure (Fig. 5) and energy levels there using XRD fitting data. Material parameters were taken from Ref. [11]. As it is seen from the CL data a piezoelectric field is observed in the sample since the spectral position of the spectra maximum depends strongly on the level of excitation. In case of high level of excitation piezoelectric field is partially screened and one can observe blue shift of spectra. Besides, presence of piezoelectric fields added reason for the suggestion of the continuous QW layers without QDs formation: generally QDs forming is accompanied by stresses relaxation in the heterostructure.

In Table 3 comparison of calculated and measured peak positions is shown. It follows from the calculations that in case of high level of excitation the piezoelectric field is

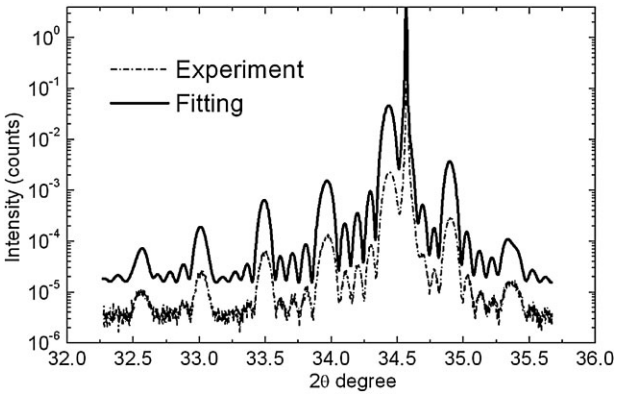

Figure 2 (a) Experimental and (b) computed diffraction curves for MQW symmetric (00.2) diffraction. The curves are shifted upward along the vertical axis for clarity.

Table 2 XRD fitting results compared to EPMA results.

layer	thickness (nm)	concentration (x)	product[a]	concentration from EPMA (x)
GaN capping	10 ± 1	–	–	–
InGaN	3.9 ± 0.4	12 ± 3	48.6	13 ± 1
GaN	16 ± 2	–	–	–
InGaN	3.0 ± 0.3	17 ± 3	49.8	17 ± 1
GaN	17 ± 2	–	–	–
InGaN	3.5 ± 0.3	15 ± 3	50.5	15 ± 1
GaN	16 ± 2	–	–	–
InGaN	3.9 ± 0.4	12 ± 3	47.6	13 ± 1
GaN	16 ± 2	–	–	–
InGaN	3.8 ± 0.4	14 ± 3	51.4	13 ± 1
GaN substrate	–	–	–	–

[a]In the fourth column the product of absolute indium atomic concentration by thickness of the layer (calculated from XRD data) is indicated.

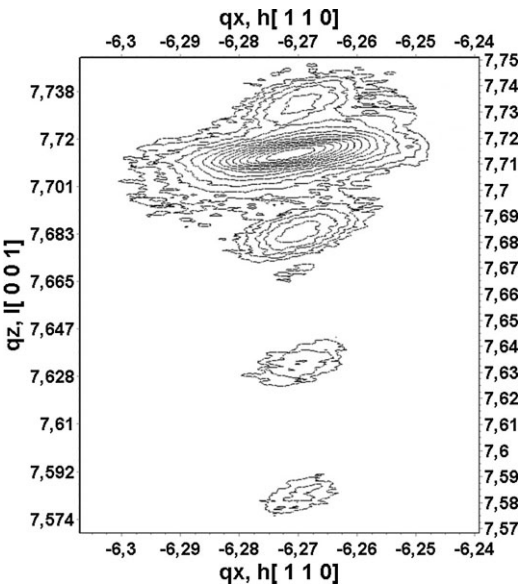

Figure 3 The experimental reciprocal-space map for MQW structure (coplanar 11.4 diffraction).

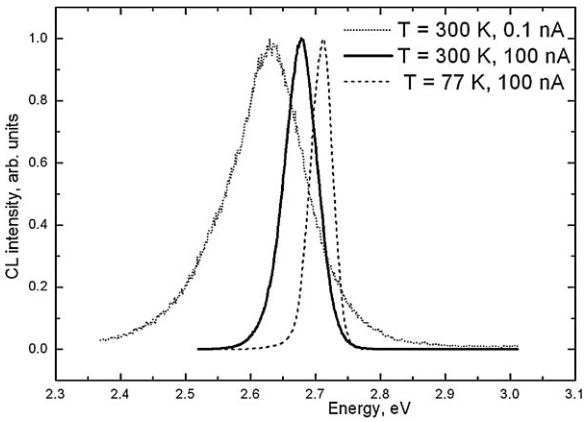

Figure 4 CL spectra of MQW sample obtained by different temperatures and levels of excitations (electron beam currents).

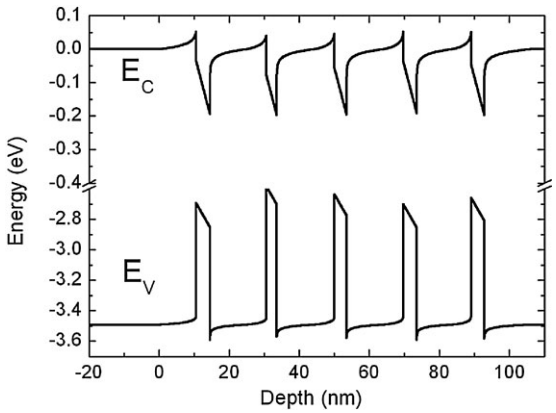

Figure 5 Calculated band structure of the MQW structure. Bottom of the conduction band counts as the zero of energy.

completely screened and can be neglected in our calculations. In other words in this case calculated energy levels based on EPMA-XRD data are in good agreement with exact position of CL spectra. If low level of excitation one has to take into account piezoelectric fields. The exact value of the piezoelectric field (145 kV/cm) was estimated from the best agreement between calculated and measured value of red shift by low level of excitation.

Table 3 Calculated and measured CL peak positions of MQW.

temperature (K)	beam current (nA)	measured peak position (eV)	calculated peak position (eV)[a]
77	0.1	2.64	2.66
77	100	2.71	2.73
300	0.1	2.63	2.63
300	100	2.68	2.68

[a]It was supposed that there is no piezoelectric field when high beam current is used.

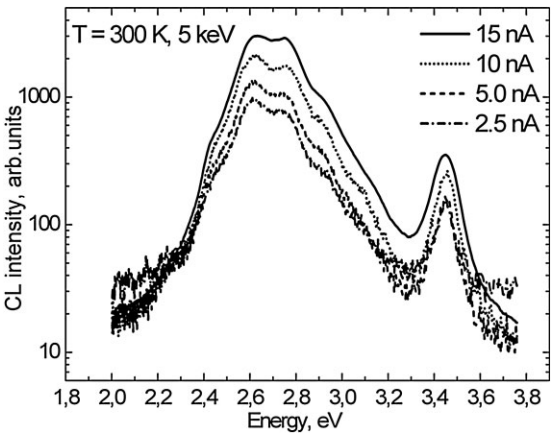

Figure 6 CL spectra of SQW sample (In-rich area) obtained by different levels of excitations (electron beam currents) at $T = 300$ K. Peak at 3.5 eV is connected with GaN buffer layer.

3.4 SQW structure TEM measurements of SQW structure showed that the QW layer decomposed into the QDs with average diameter of 5 nm. So SQW content measured by EPMA gives no information about the exact content of the QDs in the layer. Therefore, we had to use another approach.

We obtained CL spectra at different electron beam currents and did not observe any shift of the CL spectra (Fig. 6). Therefore, we made a conclusion that there is no significant impact of piezoelectric fields in this sample. Moreover, one can see that the shape of the CL spectra is complex (in contradistinction from MQW CL spectra).

We estimated the average InGaN QDs content from CL spectra. Each spectrum was fitted with Gaussians, and then the centre of the amplitude distribution was found. This average energy correlates with the average QD composition. Average content of QDs in In-rich part of the sample was estimated as In0.2Ga0.8N, in In-poor part – In0.1Ga0.9N. As a result we found that the density of QDs was comparable for both areas, being 45% for the In-rich area and 35% for the In-poor area.

4 Conclusions In this work, we have demonstrated that EPMA is a useful tool for nitride nanoheterostructures characterization. We have showed that EPMA is sensitive for measurement of very thin layers (5 nm SQW lying 120 nm under the surface).

However, it is necessary to take into account that one should be careful in EPMA result interpretation and attract additional experimental techniques. We have showed as well that CL spectra obtained at different levels of excitation give additional information about the structural perfection of quantum-sized layer.

Acknowledgements Authors would like to thank Dr. V. N. Jmerik for growing samples. The work was performed at the 'Material Science and Characterization in Advanced Technology' Joint Research Centre (St. Petersburg, Russia) and was supported

partially by the St. Petersburg Government (Grant for young researchers).

References

[1] C. Figueroa, H. Brizuela, and S. P. Heluani, J. Appl. Phys. **99**, 044909 (2006).
[2] Y. Osada, X-Ray Spectrom. **34**, 92 (2005).
[3] J.-L. Pouchou, Mikrochim. Acta **138**, 133 (2002).
[4] T. B. Popova, L. A. Bakaleinikov, E. Yu. Flegontova, and M. V. Zamoryanskaya, Mikrochim. Acta **161**, 459 (2008).
[5] S. V. Ivanov, V. N. Jmerik, T. V. Shubina, S. B. Listoshin, A. M. Mizerov, A. A. Sitnikova, M. H. Kim, M. Koike, B. J. Kim, and P. S. Kop'ev, J. Cryst. Growth **301/302**, 465 (2007).
[6] M. V. Zamoryanskaya, S. G. Konnikov, and A. N. Zamoryanskii, Instrum. Exp. Tech. **47**, 477 (2004).
[7] T. B. Popova, L. A. Bakaleĭnikov, M. V. Zamoryanskaya, and E. Yu. Flegontova, Semiconductors **2008**, 669 (2008).
[8] D. A. Kirilenko, S. A. Rukolaine, and A. A. Sitnikova, Tech. Phys. Lett. **33**(12), 1061 (2007).
[9] U. Pietsch, V. Holy, and T. Baumbach, High-Resolution X-Ray Scattering (Springer, New York, 2004), p. 408.
[10] N. N. Faleev, A. Yu. Egorov, A. E. Zhukov, A. R. Kovsh, S. S. Mikhrin, V. M. Ustinov, K. M. Pavlov, V. I. Punegov, M. Tabuchi, and Y. Takeda, Semiconductors **33**, 1229 (1999).
[11] I. Vurgaftman and J. R. Meyer, J. Appl. Phys. **94**, 6 (2003).